AJNR

Abnormalities in the Recirculation Phase of Contrast Agent Bolus Passage in Cerebral Gliomas: Comparison with Relative Blood Volume and Tumor Grade

Alan Jackson, Andrea Kassner, Deborah Annesley-Williams, Helen Reid, Xiau-Ping Zhu and Kah-Loh Li

AJNR Am J Neuroradiol 2002, 23 (1) 7-14
http://www.ajnr.org/content/23/1/7

Abnormalities in the Recirculation Phase of Contrast Agent Bolus Passage in Cerebral Gliomas: Comparison with Relative Blood Volume and Tumor Grade

Alan Jackson, Andrea Kassner, Deborah Annesley-Williams, Helen Reid, Xiau-Ping Zhu, and Kah-Loh Li

BACKGROUND AND PURPOSE: **Abnormalities in the recirculation phase of the passage of a contrast agent bolus have been identified in tumors and have been suggested to represent vascular tortuosity and hypoperfusion in areas of angiogenic neovascularization. This study was performed to examine the hypothesis that these abnormalities provide information concerning the microcirculation related to tumor grade in patients with cerebral glioma.**

METHODS: **Contrast-enhanced dynamic susceptibility MR imaging was performed in 27 patients with glioma. Residual relaxivity effects were minimized by injection of contrast agent before dynamic imaging. Maps of relative cerebral blood volume (rCBV) and relative recirculation (rR) were calculated, and values from enhancing tumor tissue were compared with tumor grade.**

RESULTS: **Histologic grades were grade II, astrocytoma (n = 3); grade III, anaplastic astrocytoma (n = 10); and grade IV, glioblastoma multiforme (n = 14). rCBV values varied among tumor grades, with higher mean values in higher grade tumors ($P < .001$). Mean rR values in grade II tumors were not significantly different from those in normal gray and white matter. Mean rR values in grades III and IV tumors were similar and were significantly higher than those in grade II tumors ($P < .01$). The distribution of the pixel values of rR showed significant differences between grades III and IV tumors ($P < .001$), with low values of skewness in keeping with a normal distribution in grade III tumors and higher values in grade IV tumors.**

CONCLUSION: **Variation in the recirculation characteristics of a contrast agent bolus is related to tumor grade in gliomas. This supports the hypothesis that abnormalities in contrast agent recirculation provide independent information concerning the microcirculation in imaging studies of angiogenesis and may be of value as surrogate markers in trials of antiangiogenic therapy.**

Tumor growth depends on the development of new blood vessels (1), which is driven by local production of angiogenic cytokines such as vasoactive endothelial growth factor (VEGF) (2). This angiogenic activity is stimulated by regional hypoglycemia and hypoxia (3), and the expression of angiogenic cytokines appears to be proportionately greater in more rapidly progressive tumors (4). Histologic examination supports this observation, and the microvascular density (MVD) of tumor tissue has been shown to relate to tumor behavior and prognosis in a wide range of tumor types (1, 5–7). Many new therapeutic agents in development target the angiogenic process either by inhibition of cytokine activity or by selective targeting of newly formed vessels (1, 8, 9). These observations have led several groups to investigate the use of MR measurements of relative cerebral blood volume (rCBV) as a possible in vivo marker related to MVD (6, 10–13). A number of MR studies have shown strong correlation between rCBV and both histologic vascularity and tumor grade (6, 13), and one study showed rCBV responses to antiangiogenic doses of thalidomide and carboplatin (14). Capillary perme-

Received March 9, 2001; accepted after revision July 30.

From Imaging Science and Biomedical Engineering, University of Manchester, Manchester (A.J. D.A-W., X-P.Z., K-L.L.); Philips Medical Systems, Hammersmith, London (A.K.); and Department of Neuropathology, Hope Hospital, Salford (H.R.), United Kingdom.

Address reprint requests to Professor Alan Jackson, University of Manchester, Imaging Science and Biomedical Engineering, Stopford Building, Oxford Road, Manchester M13 9PT, United Kingdom.

ability is also elevated in neoangiogenic vasculature as a direct effect of cytokine activation. MR measurements of endothelial permeability have been shown to correlate with histologic grade in glioma (15) and have been proposed as a surrogate marker of antiangiogenic drug activity.

In a previous publication (16), we examined changes in the recirculation phase of the first passage of a contrast agent bolus in tumors due to disruption of normal flow patterns by chaotic tumoral vasculature. We described a new parameter, relative recirculation (rR), to allow quantification of abnormalities in the recirculation phase. The rR provides a quantitative indicator of delayed local passage of intravascular contrast agent through the microvasculature. We previously demonstrated elevated areas of rR in a range of cerebral tumors and showed that this occurred independent of local variations in rCBV (16). The changes were observed only in those regions of tumor in which histologic studies would help predict increased neovascularization and vascular complexity. On the basis of this evidence, together with simple mathematical modeling of the effects of microvascular structure on the shape of the contrast agent bolus, we propose that rR indicates abnormal flow patterns that can result from vascular tortuosity and variations in regional perfusion pressure (16).

The biologic value of rR measurements remains to be clarified, and the role, if any, of the measurement in clinical practice is not yet clear. However, on the basis of our previous observations, it is apparent that elevation of rR occurs independent of elevations in rCBV and is more common in rapid-growing tumors (16). The measurement helps identify areas of delayed flow such as are seen in hypoperfused areas of gliomas in which the anoxic and hypoglycemic stimulus for the production of angiogenic cytokines is greatest (3, 16). The measurement of rR could therefore provide an indicator of the extent and location of active angiogenic activity, which may be of value as a surrogate marker in the development and testing of novel antiangiogenic therapies. The measurement may also be valuable in identifying areas of maximal angiogenic drive for image-guided biopsy to allow histologic quantification of maximal angiogenic activity within the tumor based on measurements of cytokine expression, such as receptor density.

To assess the potential value of rR as a marker of angiogenic activity, it is important that we further characterize the behavior of this variable. This study was designed to examine the relationship among these abnormalities of the recirculation phase, rCBV, and histologic grade in a series of patients with cerebral glioma to test the hypothesis that abnormalities of rR will correlate with tumor grade.

Methods

Research Subjects

The study was approved by the Manchester Local Research Ethics Committee. All patients gave informed consent before inclusion and underwent diagnostic MR or CT examinations before recruitment. Twenty-seven patients (16 men, 11 women; median age, 56 years; age range, 34–72 years) suspected to have glioma were included in the study.

Histologic Analysis

All patients underwent tumor biopsy (n = 12) or debulking (n = 15) within 4 days of the imaging study. Tissue samples were retrospectively reviewed by a neuropathologist (H.R.) specializing in cerebral tumors, who was blinded to the imaging results. Histologic analysis was performed on hematoxylin-eosin–stained sections, and tumors were classified according to the revised World Health Organization classification of 1993 (17).

Image Acquisition

In all 27 patients, an enhancing mass lesion was depicted on either CT or MR images before inclusion in the study. All imaging was performed within 5 days of presentation, before biopsy or definitive treatment, although all patients were receiving steroids to reduce intracranial pressure. Imaging was performed by using a 1.5-T whole-body MR system (Phillips ACS NT6000; Phillips Medical Systems, Best, the Netherlands) (maximum gradient strength, 23 mT/M; maximum slew rate, 105 mT/M/ms) with a birdcage head coil. Before imaging, a 16–18-gauge catheter was inserted into an antecubital vein, and a local anesthetic was administered. The larger needle bore was initially employed to minimize resistance to manual injection; however, adequate injection rates can be attained by using an automated injection pump with an 18-gauge needle. Routine clinical T1- and T2-weighted imaging was performed in all patients before dynamic studies. Perfusion imaging was performed by using a multisection field-echo echo-planar sequence with heavy T2* weighting (262/30 [TR/TE], 35° flip angle, matrix 128 × 128). A gradient-echo technique was preferred over the spin-echo sequence to avoid spurious suppression of signal changes in large vessels (18, 19). The acquisition collected 9 × 5-mm-thick sections with an intersection gap of 0.5 mm. The temporal resolution was 1.89 seconds per acquisition, and a series of 60 consecutive acquisitions were obtained. Contrast agent (0.1 mmol/L gadodiamide injection [Omniscan; Nycomed, Oslo, Norway]) was injected 10 minutes before imaging to remove residual relaxivity effects. The interval of 10 minutes was based on a published study (16) from our laboratory designed to identify the optimal method for the removal of residual relaxivity effects in T2*-weighted data. A subsequent dose of contrast agent (0.1 mmol/L gadodiamide injection) was administered during image acquisition after the 10th dynamic image was obtained (t = 1.86 seconds). The injection was made over 4 seconds and was followed by a chaser of 35 mL of normal saline at the same rate. Injections in the first 16 patients were performed with a manual injection technique. Manual injections were made by a single experienced operator (A.J.) with use of a metronome to control injection timing and a large-bore (16-gauge) needle for all manual injections. In the subsequent 11 patients, injections were made with an automated power injector (Spectris; Medrad). Images were transferred to an independent workstation for analysis.

Calculation of Parametric Images

Perfusion data sets were used to calculate T2* rate changes (Δ R2) with the relationship

$$\Delta R2 = -\ln(S_{(t)}/S_{(0)})/TE, \quad (1)$$

where $S_{(0)}$ is the baseline signal intensity, $S_{(t)}$ is the pixel intensity at time t, and TE is the echo time (20).

To produce a theoretical first-pass curve free of recirculation effects, the data were fitted to a gamma variant function by using a Simplex curve-fitting algorithm with the relationship

$$\Delta R2_{(t)} = Q(t^r)\exp(-t/b) \quad (2)$$

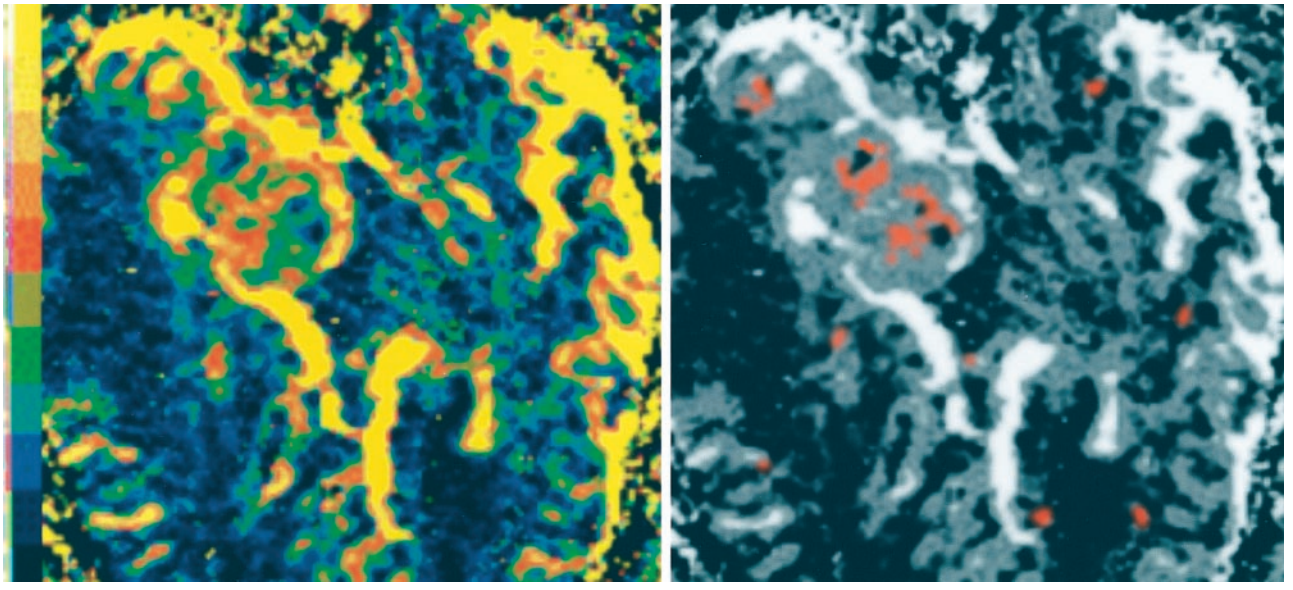

FIG 1. Parametric images of rCBV (*left*) and rR (*right*) in a patient with glioblastoma multiforme. The rCBV map is in color to aid interpretation. The color scale is nonlinear: *black*, ≤2%; *blue*, 2–5%; *green*, 5–10%; *red*, 10–30%; *orange*, 30–80%; and *yellow*, ≥80%. The image demonstrates large peripheral vessels (*yellow*) and a central area of high rCBV within the tumor core (*red*) and other central areas of poor perfusion or necrosis (*black*). The *red* areas in the rR map indicate pixels with values <0.46, which are seen in fewer than 2% of normal tissue. Single-pixel areas of elevated rR have been filtered out, and the pixel clusters have been filtered by using a 0.5-pixel gaussian filter. The underlying gray-scale image shows the rCBV map. This image demonstrates areas of elevated rR, which occur principally in the center of the tumor, adjacent to areas of necrosis and away from the central area of elevated rCBV.

where Q, r, and b are fitting constants (21, 22).

Curve-fitting data were used to derive parametric maps of rCBV, which is proportional to the area under the Δ R2 curve. This was calculated analytically as

$$3) \qquad rCBV = \int_{t_0}^{t_e} \Delta R2(t)dt,$$

where t_0 is the time of first arrival of contrast agent and t_e is the time at which Δ R2 returns to baseline.

Curve fitting and derivation of calculated images were performed with a software program developed in Interactive Data Language (Floating Point Software; Research System Software Ltd, Boulder, CO) and C. This program calculated the fitting constants Q, r, and b by using a "down-hill" Simplex method (23, 24).

The recirculation phase of the time-signal response curve was examined by calculation of the area between the ideal first-pass curve represented by the gamma variate function and the measured data during the recirculation phase. The measurement was made between the midpoint of the down-slope of the gamma variate fit and a point 30 seconds after the initial contrast agent arrival time (t_0). Because the area under the time-intensity curve partially represents true contrast agent recirculation (25), it would be predicted to correlate closely with regional rCBV. To remove this correlation, the recirculation parameter was normalized by using the maximum value of ΔR2 ($\Delta R2_{max}$). This normalized parameter, rR, was calculated on a voxel-by-voxel basis and used to construct parametric maps as follows:

$$4) \qquad rR = \frac{\sum_{i=A}^{N} (\Delta R2_{measured}(i) - \Delta R2_{theoretical}(i))}{\Delta R2_{max}(N - A)},$$

where $\Delta R2_{max}$ is the maximum value of $\Delta R2_{theoretical}$

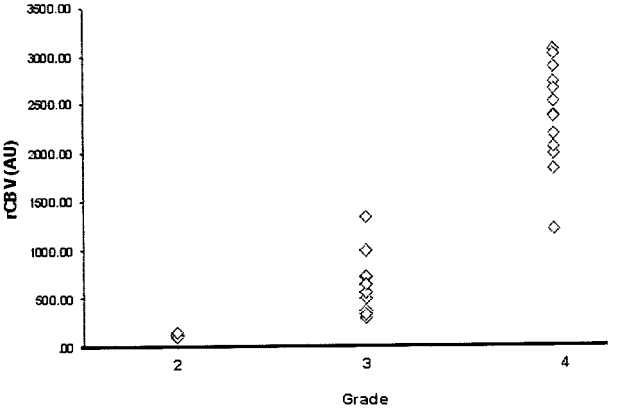

FIG 2. Plot of mean rCBV values against tumor grade shows increase in rCBV with increasing tumor grade. (*AU* indicates arbitrary units.)

Image Analysis

Enhancing tumor tissue was manually segmented from post-contrast T1-weighted images by an experienced neuroradiologist (A.J.), and the resultant volumes of interest (VOIs) were transferred to corresponding parametric maps of rCBV and rR. VOIs included only enhancing tissue. The pixel values from these VOIs were exported to ASCII files, and the relationship between tumor grade and the parametric variables was examined by using standard statistical software packages.

Although indicators of distribution position (mean or median) are traditionally used in this type of analysis, it is important to remember that regional abnormalities in microvascular structure may affect only a small proportion of the tumor pixels and may preferentially affect those with high or low values (26). Because abnormalities in the rR parameter have previously been shown to affect only a small proportion of the tumor (16), a number of parameters reflecting the distribution of rR and rCBV were calculated for each tumor to examine variations in both the position and shape of the pixel distributions. Param-

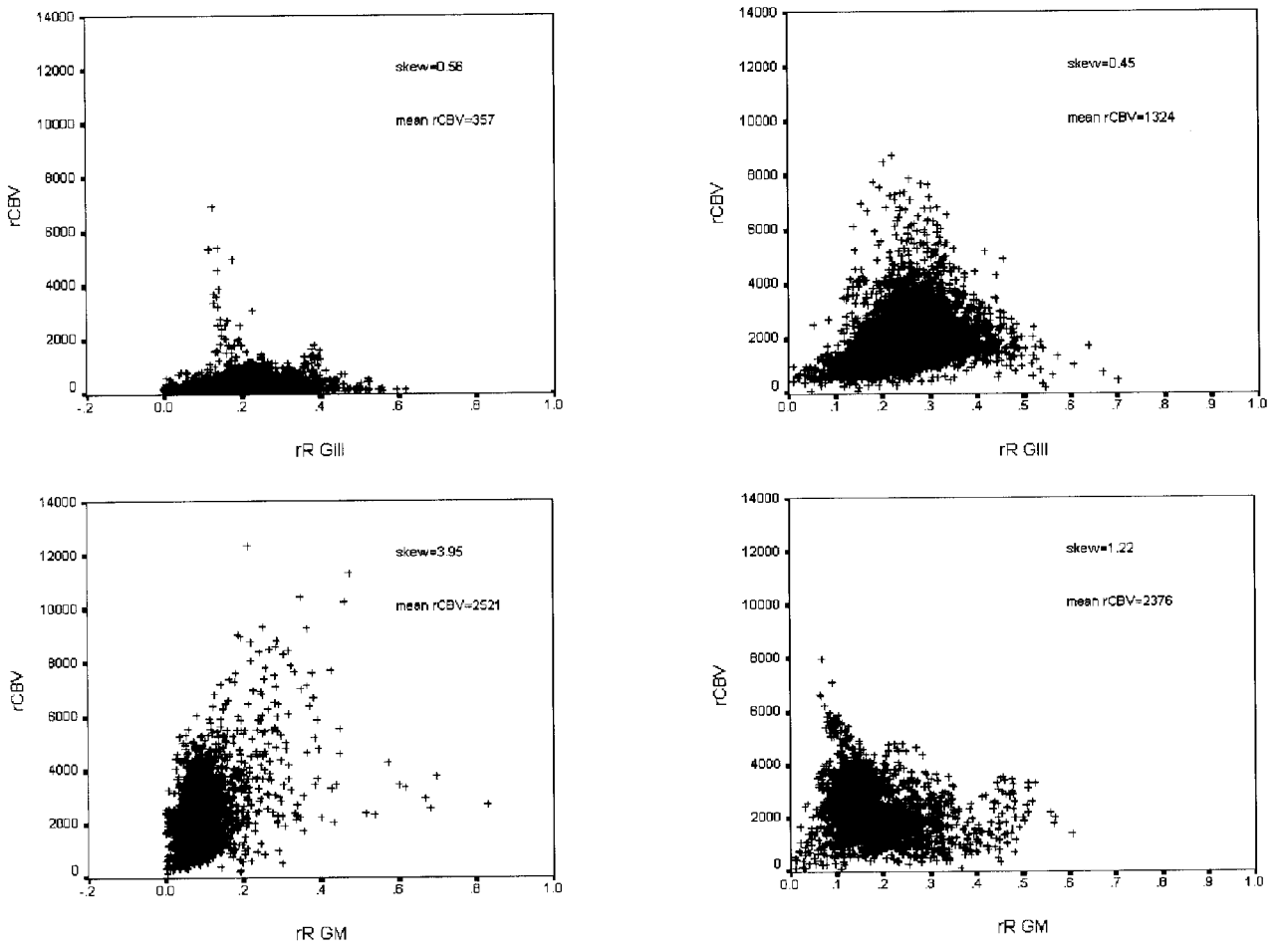

FIG 3. Pixel-by-pixel plots of rR versus rCBV for two examples of anaplastic astrocytoma (*GIII*) (*top*) and glioblastoma multiforme (*GIV*) (*bottom*). rR values show a relatively normal distribution in the grade III tumors and a more skewed distribution in the grade IV tumors. No evidence of correlation exists between rCBV and rR.

eters included mean values to identify any shift in the overall position of the pixel distribution; 95%, 90%, 85%, and 80% values to identify any changes in the distribution of high values; and the skewness of the distribution to identify any changes in the shape of the pixel distribution that might result from a change in pixel values within the lower 80%. Skewness was calculated as follows: (mean − mode)/SD. Comparisons with tumor grade were made with a one-way analysis of variance. A *P* value less than .05 indicated a statistically significant difference.

Results

Histologic data were available from biopsy (n = 12) or excision samples (n = 15) in all cases. Histologic analysis confirmed the suspected diagnosis of glioma in all cases. Histologic gradings were grade II, astrocytoma, in three patients; grade III, anaplastic astrocytoma, in 10 patients; and grade IV, glioblastoma multiforme, in 14 patients.

Dynamic images showed no evidence of significant motion during data acquisition in any case, and parametric images of rCBV and rR were of high quality (Fig 1). Measurements of mean rCBV (in arbitrary units) from the VOI ranged from 102 to 3256 with a group mean of 1678. The range of measurements for the mean rR was 0.076–0.257 with a group mean of

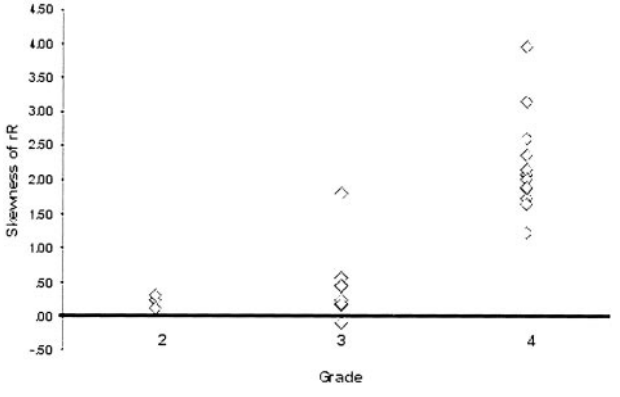

FIG 4. Plot of skewness of rR against tumor grade shows increased skewness in grade IV tumors.

0.156. In normal tissue, values of rR exceeded 0.35 in 5% of pixels and 0.46 in fewer than 2%. Elevated values of rR above these thresholds were seen in two of the three grade II tumors with 7% and 9.6% of pixels above 0.35 and less than 1% of pixels above 0.46. Elevated values of rR were seen in all grades III and IV tumors with 9–21% of pixels above 0.35 and 8–12% above 0.46. Elevation of rR was most com-

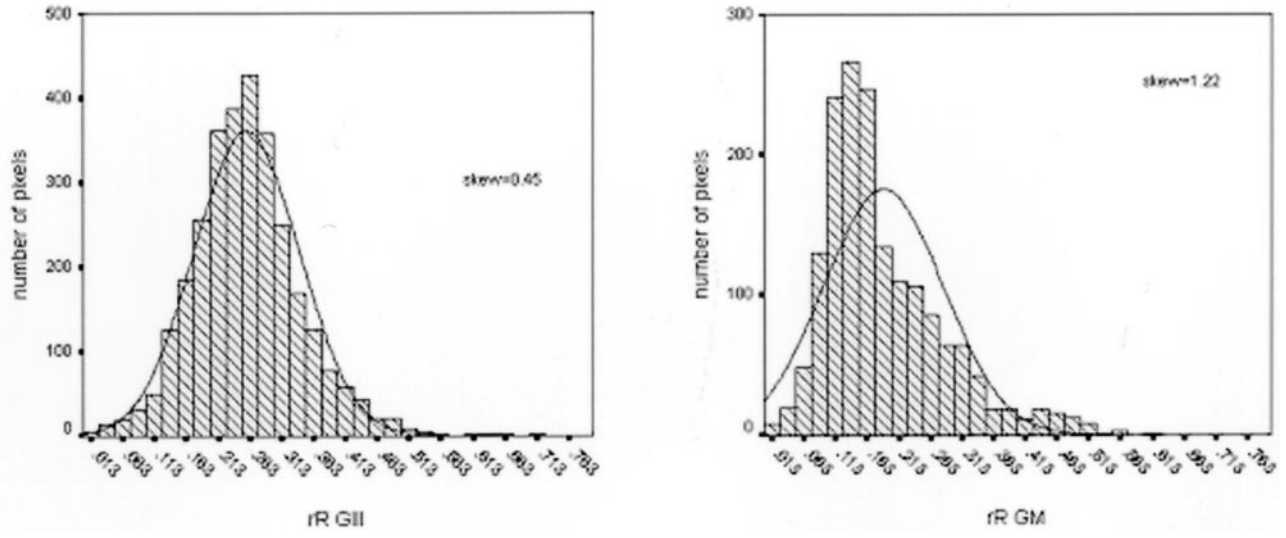

FIG 5. Plot of rR values in one patient with a grade III tumor (*left*) and one patient with a grade IV tumor (*right*) shows loss of conformance of the pixel values to the normal distribution in the grade IV tumor. The optimal fitted normal distribution is illustrated.

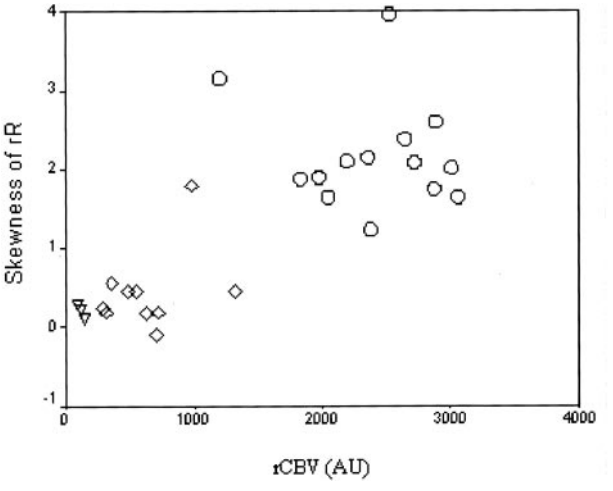

FIG 6. Plot of skewness of rR against mean rCBV values demonstrates the separation of grade IV tumors on the basis of both skewness of rR and rCBV and the separation of grade II and grade III tumors by rCBV. Grade II tumors are represented by triangles, grade III by diamonds, and grade IV by circles. (*AU* indicates arbitrary units.)

monly seen in the central area of the tumors and adjacent areas of central necrosis, as previously described (16). The frequency of elevated values in grade II tumors was not significantly different than that of values in normal gray and white matter. Values in grades III and IV tumors were significantly greater than in grade II tumors and normal tissue ($P < .01$). No significant difference in the prevalence of elevated values existed between grades III and grade IV tumors.

Values of rCBV varied with tumor grade, with higher mean values seen in higher grade tumors (Fig 2, $P < .001$). Use of the 95–75% points for rCBV and rR, as an indicator of distribution shape, confirmed a significant increase in pixels above these thresholds in grades III and IV tumors compared with those in grade II tumors but showed no significant difference between grade III and grade IV tumors. The skewness of the distribution of rCBV was not related to tumor grade. Skewness of the distributions of rR showed no difference between grade II and grade III tumors; both demonstrated low values, in keeping with a normal distribution. Grade IV tumors demonstrated greater skewness in the distribution of rR, not in keeping with a normal distribution (Figs 3–5) and significantly greater values than in grade II and grade III tumors ($P < .001$). Although the number of patients in the study is small, a plot of the skewness of rR against mean rCBV values (Fig 6) suggests that these parameters provide complementary information about tumor microvasculature, both of which are independently related to tumor grade.

Discussion

The angiogenic process is central to tumor growth and provides a target for novel therapeutic approaches (1, 8, 9). The development and application of these new antiangiogenic therapies is highly dependent on the identification of surrogate markers of angiogenic activity, and many groups have studied the use of MR-based techniques to characterize and quantify the angiogenic neovasculature (12, 14, 15, 26). The microvascular structure that develops in tumors in response to angiogenic cytokine activity differs in many ways from that seen in normal tissue (27). These abnormalities of arterial and venous structures are well known to pathologists who identify features such as vascular complexity and dysplasia to support tumor classification. Abnormalities in the tumor vasculature are found in all components of the vascular tree including the capillary structure, and the severity of the disorganization generally correlates with growth rate and malignant behavior. These areas of abnormal structure are associated with an increased proportion of vessels and with increased tortuosity of the vessels themselves (28, 29). Both of

these factors relate to histologic measurements of MVD, which can be increased by the presence of increased numbers of vessels and by the presence of tortuous vessels that repeatedly pass through the plane of the section.

The development of MR-based surrogate measures of angiogenic activity may have considerable impact in the determination of tumor grade, prognosis, metastatic potential, therapeutic response, and tumor recurrence (6, 26, 30–33). The measurement of rCBV provides an obvious surrogate for estimations of MVD and has shown good correlation with both grade and prognosis in a range of tumor types (12, 15, 34). The findings in this study were in close agreement with those of previous investigators who demonstrated a significant increase in mean values of rCBV in high-grade tumors (Fig 1). Technically, the measurement of rCBV in tumors is complicated where there is breakdown of the blood-brain barrier. Measurements based on relaxivity effects will reflect a combination of first-pass kinetics and contrast agent leakage into the extracellular space (35). Imaging sequences sensitive to susceptibility effects will reveal a decrease in signal intensity because of contrast agent passage. However, any sensitivity to relaxivity effects will cause elevation of signal intensity (T1 shine-through), which may result in underestimation of rCBV (6, 36). We previously compared a number of techniques to reduce this T1 shine-through (16) and found preenhancement of the tumor by administration of a dose of contrast agent 5–10 minutes before the dynamic imaging sequence to be highly effective at removing T1 shine-through. This approach also allows the use of high-flip-angle techniques, with consequent improvements in signal-to-noise ratio of the T2*-dependent signal intensity change, which allows us to measure the abnormalities in the recirculation phase.

Measurement of capillary endothelial permeability with MR imaging of contrast agent distribution also provides information about the angiogenic process, because angiogenic cytokines, such as VEGF, are rapid and potent promoters of endothelial permeability (37). Previous investigators have been able to show a relationship between endothelial permeability and grade in gliomas (15) and to show rapid decreases in endothelial permeability over 24 hours in response to anti-VEGF therapy in a range of tumor types (38). The information provided by measurements of rCBV and endothelial permeability is complementary, with rCBV providing an indication of the amount of neoangiogenic vessel formation that has occurred and endothelial permeability providing an indicator of the current cytokine activity within the tumor. The ability of endothelial permeability measurements to reveal major changes within hours of first administration of angiogenic cytokine blockers (38) provides a powerful tool for the development and testing of antiangiogenic agents.

Abnormalities in the recirculation phase of the contrast agent bolus also offer the possibility of further characterizing the neoangiogenic microvasculature. The angiogenic process is stimulated by regional hypoxia and hypoglycemia (3); thus, cytokine production is most active in areas of the tumor subject to hypoperfusion and ischemia. In rapidly growing tumors such as glioblastoma multiforme, the angiogenic activity is unable to provide adequate perfusion, and necrosis occurs in central areas of the tumor. The areas of most active angiogenic cytokine production are characterized by inadequate perfusion, and capillary blood flow is likely to be slow and erratic (27). These flow characteristics will give rise to the abnormalities in the recirculation phase of the contrast agent bolus, which we have demonstrated herein and in previous work (16). The rR parameter therefore can indicate these areas of inadequate and deranged flow that likely exist deep in the tumor and adjacent to areas of necrosis. The finding of these abnormalities is likely to indicate a rapidly growing, aggressive tumor in which the angiogenic process is failing to adequately support tumor demands. These hypotheses are supported by the finding of elevated areas of rR centrally within glioblastomas in areas adjacent to regions of necrosis ([16] and Fig 1) and by the observation in this study that elevation of rR is seen only in grade III and IV tumors.

Because the role of the angiogenic process is to ensure adequate perfusion to the tumor tissue, it is unlikely that slow-growing tumors will contain areas of significant hypoperfusion. In more rapidly growing tumors, we can expect areas in which perfusion pressure is low and blood flow is sluggish and disorganized, leading to abnormalities in the recirculation phase. As discussed above, these effects are likely to be most marked deep in the tumor in areas furthest from the supplying vessels. However, it is also possible that similar flow disruption will occur, albeit to a lesser extent, in more superficial areas of the tumor. The increase in mean rR in grade III and IV tumors supports the suggestion that changes in rR are associated with widespread abnormality affecting many of the tumor pixels. However, the similarity in mean rR values between grade III and IV tumors does not exclude a difference in the circulatory properties between them. Measurements of skewness of the pixel distribution of rR demonstrated a clear variation between grade III and grade IV tumors. Skewness is a measure of the asymmetry of a distribution. The normal distribution is symmetric and has a skewness value of zero. A distribution with a significant positive skewness has a long right tail. A distribution with a significant negative skewness has a long left tail. A skewness value greater than 1 generally indicates that the data differ significantly from a normal distribution. In the current study, nine of 10 grade III tumors demonstrated a skewness of the distribution of rR that was less than 1, whereas all grade IV tumors demonstrated values between 1 and 4.5. This finding indicates a shift in the distribution of rR values so that the higher grade tumors have a greater proportion of voxels, with values above the mode of the distribution. These observations suggest that the presence of increased areas of slow or deranged perfusion in grade IV tumors produces a significant increase in rR in

many voxels. This change is insufficient to further affect the mean values of the distribution but does shift sufficient voxels to produce a significant skewness in the distribution. This observation is of considerable interest for two reasons. First, it supports our hypothesis that abnormalities in the recirculation phase, as demonstrated by rR, reflect tumor grade and that increases in rR are seen in higher grade disease. Second, these observations indicate that the use of simple measures such as the mean of a distribution can be insensitive in detecting changes in parametric variables. This has been noted by Mayr and colleagues (26), who used measurements of dynamic contrast enhancement in cervical carcinoma. In their investigation, a highly heterogeneous distribution of enhancement pattern was seen, and the incidence of tumor recurrence was best predicted by the value of the lower centiles of the distribution. These investigators suggest that this might reflect the higher recurrence rates in hypoxic tumors after radiation therapy. Their findings suggest that low-grade (grade II) tumors maintain normal perfusion patterns indistinguishable from those in normal tissue but that more aggressive tumors (grades III and IV) are marked by abnormal flow affecting most of the tumor tissue. This abnormal flow results in an increase in the mean rR. In grade IV tumors that are histologically characterized by areas of necrosis, no increase in the mean or in the high rR values exists, but more of the pixels within the tumor show abnormal elevation of rR, resulting in a change in the pixel distribution. The distribution of markedly elevated values of rR can be seen on parametric images (Fig 1). However, the skewness of the distribution can only be detected by analysis of all the tumor pixel values and cannot be represented as a pixel-by-pixel map.

The clinical role of the rR parameter still requires further elucidation. It is likely that parametric maps of elevated rR would help in the distinction between grade I and II gliomas and those of higher grade. However, it is unlikely that this would improve diagnostic accuracy over simple measurements of rCBV or endothelial permeability. In grades III and IV tumors, parametric maps will allow the identification of areas of abnormal perfusion that could be used to guide biopsy procedures to improve the identification of areas of dedifferentiation within grade II tumors and avoid histologic undergrading. One grade III tumor in the current study demonstrated a high skewness of rR (Fig 6), although rCBV values were in keeping with a grade III tumor. The use of the rR map in this case may have allowed more specific biopsy of an area of dedifferentiation and may have led to a change in histologic grading. However, the most likely clinical role for the rR parameter in gliomas is in the development and use of novel antiangiogenic therapies. The gliomas are heavily expressive of VEGF, which appears to be the dominant stimulus of angiogenesis in this tumor line. The rR measurement provides a potential surrogate marker of response to antiangiogenic therapies capable of identifying subtle changes in perfusion characteristics that may result from inhibition of new vessel development. It could also provide an indicator of microvascular flow disruption resulting from therapies such as microtubulin poisons that change tumor perfusion pressure by damaging the neovasculature.

Conclusion

We have shown that abnormalities of the recirculation phase of a contrast agent bolus can be demonstrated in high-grade gliomas and are not seen in lower grade tumors. Parametric maps of rR can be used to identify areas of disorganized flow, which may be useful in guiding stereotactic biopsy in higher grade tumors. In higher grade tumors, increasing grade is accompanied by changes in the distribution of rR that are characterized by a skewness in the distribution of the rR parameter. We suggest that rR may have a role in the development and monitoring of novel antiangiogenic therapies.

References

1. Endrich B, Vaupel P. **The role of the micro-circulation in the treatment of malignant tumours: facts and fiction.** In: Molls M, Vaupel P, eds. *Blood Perfusion and Microenvironment of Human Tumours.* Berlin-Heidelberg: Springer; 1998:19–39
2. Amoroso A, Del Porto F, Di Monaco C, Manfredini P, Afeltra A. **Vascular endothelial growth factor: a key mediator of neoangiogenesis—a review.** *Eur Rev Med Pharmacol Sci* 1997;1:17–25
3. Shweiki D, Neeman M, Itin A, Keshet E. **Induction of vascular endothelial growth factor expression by hypoxia and by glucose deficiency in multicell spheroids: implications for tumor angiogenesis.** *Proc Natl Acad Sci U S A* 1995;92:768–772
4. Jensen RL. **Growth factor-mediated angiogenesis in the malignant progression of glial tumors: a review.** *Surg Neurol* 1998;49:189–195 [See comments 1998;49:196.]
5. Brem S, Cotran R, Folkman J. **Tumour angiogenesis: a quantitative method for histological grading.** *J Natl Cancer Inst* 1972;28:347–356
6. Aronen HJ, Gazit IE, Louis DN, et al. **Cerebral blood volume maps of gliomas: comparison with tumor grade and histologic findings.** *Radiology* 1994;191:41–51
7. Weidner N, Folkman J. **Tumoral vascularity as a prognostic factor in cancer.** *Important Adv Oncol* 1996;167–190
8. Dachs GU, Chaplin DJ. **Microenvironmental control of gene expression: implications for tumor angiogenesis, progression, and metastasis.** *Semin Radiat Oncol* 1998;8:208–216
9. Winlaw DS. **Angiogenesis in the pathobiology and treatment of vascular and malignant diseases.** *Ann Thorac Surg* 1997;64:1204–1211
10. Miyati T, Banno T, Mase M, et al. **Dual dynamic contrast-enhanced MR imaging.** *J Magn Reson Imaging* 1997;7:230–235
11. Maeda M, Itoh S, Kimura H, et al. **Vascularity of meningiomas and neuromas: assessment with dynamic susceptibility-contrast MR imaging.** *AJR Am J Roentgenol* 1994;163:181–186
12. Aronen HJ, Glass J, Pardo FS, et al. **Echo-planar MR cerebral blood volume mapping of gliomas: clinical utility.** *Acta Radiol* 1995;36:520–528.
13. Griebel J, Mayr NA, de Vries A, et al. **Assessment of tumor microcirculation: a new role of dynamic contrast MR imaging.** *J Magn Reson Imaging* 1997;7:111–119
14. Cha S, Knopp EA, Johnson G, et al. **Dynamic contrast-enhanced T2-weighted MR imaging of recurrent malignant gliomas treated with thalidomide and carboplatin.** *AJNR Am J Neuroradiol* 2000;21:881–890
15. Roberts HC, Roberts TP, Brasch RC, Dillon WP. **Quantitative measurement of microvascular permeability in human brain tumors achieved using dynamic contrast-enhanced MR imaging: correlation with histologic grade.** *AJNR Am J Neuroradiol* 2000;21:891–889
16. Kassner A, Annesley DJ, Zhu XP, et al. **Abnormalities of the contrast re-circulation phase in cerebral tumors demonstrated using dynamic susceptibility contrast-enhanced imaging: a possi-**

ble marker of vascular tortuosity. *J Magn Reson Imaging* 2000;11: 103–113
17. Kleihues P, Burger PC, Scheithauer BW. *Histological Classification of CNS Tumours of the Central Nervous System,* 2nd ed. Berlin: Springer-Verlag; 1993: 1–105
18. Weisskoff RM, Zuo CS, Boxerman JL, Rosen BR. **Microscopic susceptibility variation and transverse relaxation: theory and experiment.** *Magn Reson Med* 1994;31:601–610
19. Boxerman J, Hamberg L, Rosen B, Weisskoff R. **MR contrast due to intravascular magnetic susceptibility perturbations.** *Mag Reson Med* 1995;34:555–566
20. Rosen BR, Belliveau JW, Vevea JM, Brady TJ. **Perfusion imaging with NMR contrast agents.** *Magn Reson Med* 1990;14:249–265
21. Boxerman JL, Rosen BR, Weisskoff RM. **Signal-to-noise analysis of cerebral blood volume maps from dynamic NMR imaging studies.** *J Magn Reson Imaging* 1997;7:528–537
22. Benner T, Heiland S, Erb G, Forsting M, Sartor K. **Accuracy of gamma-variate fits to concentration-time curves from dynamic susceptibility-contrast enhanced MRI: influence of time resolution, maximal signal drop and signal to noise.** *Magn Reson Imaging* 1997;15:307–317
23. Buckley DL, Kerslake RW, Blackband SJ, Horsman A. **Quantitative analysis of multi-slice Gd-DTPA enhanced dynamic MR images using a Simplex minimization procedure.** *Magn Reson Med* 1994;32:646–651
24. Press W, Teukolsky S, Vetterling W, Flannery B. **Minimization or maximization of functions**. In: *Numerical Recipes in C: The Art of Scientific Computing*. New York: Cambridge University Press; 1992: 394–454
25. Rosen BR, Belliveau JW, Aronen HJ, et al. **Susceptibility contrast imaging of cerebral blood volume: human experience.** *Magn Reson Med* 1991; 22:293–299
26. Mayr N, Hawighorst H, Yuh W, et al. **MR microcirculation assessment in cervical cancer: correlations with histomorphological tumour markers and clinical outcome.** *J Magn Reson Imaging* 1999; 10:267–276
27. Konerding M, van Ackern C, Fait E, Steinberg F, Streffer C. **Morphological aspects of tumour angiogenesis and microcirculation.** In: Molls M, Vaupel P, eds. *Blood Perfusion and Microenvironment of Human Tumours.* Berlin-Heidelberg: Springer; 1998: 5–17
28. Plate K, Mennel H. **Vascular morphology and angiogenesis in glial tumours.** *Exp Toxic Pathol* 1995;47:89–94
29. Plate KH, Risau W. **Angiogenesis in malignant gliomas.** *Glia* 1995; 15:339–347
30. Zetter BR. **Angiogenesis and tumor metastasis.** *Annu Rev Med* 1998;49:407–424
31. Mayr NA, Yuh WT, Zheng J, et al. **Prediction of tumor control in patients with cervical cancer: analysis of combined volume and dynamic enhancement pattern by MR imaging.** *AJR Am J Roentgenol* 1998;170:177–182
32. Wenz F, Rempp K, Hess T, et al. **Effect of radiation on blood volume in low-grade astrocytomas and normal brain tissue: quantification with dynamic susceptibility contrast MR imaging.** *AJR Am J Roentgenol* 1996;166:187–193
33. Bruening R, Kwong KK, Vevea MJ, et al. **Echo-planar MR determination of relative cerebral blood volume in human brain tumors: T1 versus T2 weighting [see comments].** *AJNR Am J Neuroradiol* 1996;17:831–840
34. Siegal T, Rubinstein R, Tzuk-Shina T, Gomori JM. **Utility of relative cerebral blood volume mapping derived from perfusion magnetic resonance imaging in the routine follow up of brain tumors.** *J Neurosurg* 1997; 86:22–27
35. Hacklander T, Reichenbach JR, Modder U. **Comparison of cerebral blood volume measurements using the T1 and T2* methods in normal human brains and brain tumors.** *J Comput Assist Tomogr* 1997; 21:857–866
36. Edelman RR, Mattle HP, Atkinson DJ, et al. **Cerebral blood flow: assessment with dynamic contrast-enhanced T2*-weighted MR imaging at 1.5 T.** *Radiology* 1990;176: 211–220
37. Dvorak HF, Brown LF, Detmar M, Dvorak AM. **Vascular permeability factor/vascular endothelial growth factor, microvascular hyperpermeability, and angiogenesis.** *Am J Pathol* 1995;146:1029–1039
38. Jayson G, Mulatero C, Ranson M, et al. **Anti-VEGF antibody HuMV833: an EORTC biological treatment development group phase I toxicity: pharmacokinetic and pharmacodynamic study.** *In: Proceedings of the American Society of Clinical Oncology, San Francisco, Ca,* 2001